

## Triple $\alpha$ -particle resonances in the decay of hot nuclear systems\*

S. Zhang(张苏雅拉吐)<sup>1,1)</sup> J. C. Wang(王金成)<sup>1</sup> A. Bonasera<sup>2,3</sup> M. R. Huang(黄美容)<sup>1</sup> H. Zheng(郑华)<sup>4</sup>  
G. Q. Zhang(张国强)<sup>5,6</sup> Z. Kohley<sup>2,7</sup> Y. G. Ma(马余刚)<sup>6,8</sup> S. J. Yennello<sup>2,7</sup>

<sup>1</sup>College of Physics and Electronics information, Inner Mongolia University for Nationalities, Tongliao 028000, China

<sup>2</sup>Cyclotron Institute, Texas A&M University, College Station, Texas 77843, USA

<sup>3</sup>Laboratori Nazionali del Sud, INFN, via Santa Sofia, 62, 95123 Catania, Italy

<sup>4</sup>School of Physics and Information Technology, Shaanxi Normal University, Xi'an 710119, China

<sup>5</sup>Shanghai Advanced Research Institute, Chinese Academy of Sciences, Shanghai 201210, China

<sup>6</sup>Shanghai Institute Applied Physics, Chinese Academy of Sciences, Shanghai 201800, China

<sup>7</sup>Chemistry Department, Texas A&M University, College Station, Texas 77843, USA

<sup>8</sup>Key Laboratory of Nuclear Physics and Ion-beam Application (MOE), Institute of Modern Physics, Fudan University, Shanghai 200433, China

**Abstract:** The Efimov (Thomas) trimers in excited  $^{12}\text{C}$  nuclei, for which no observation exists yet, are discussed by means of analyzing the experimental data of  $^{70(64)}\text{Zn}(^{64}\text{Ni}) + ^{70(64)}\text{Zn}(^{64}\text{Ni})$  reactions at the beam energy of  $E/A = 35$  MeV/nucleon. In heavy ion collisions,  $\alpha$ -particles interact with each other and can form complex systems such as  $^8\text{Be}$  and  $^{12}\text{C}$ . For the 3  $\alpha$ -particle systems, multi-resonance processes give rise to excited levels of  $^{12}\text{C}$ . The interaction between any two of the 3  $\alpha$ -particles provides events with one, two or three  $^8\text{Be}$ . Their interfering levels are clearly seen in the minimum relative energy distributions. Events with the three  $\alpha$ -particle relative energies consistent with the ground state of  $^8\text{Be}$  are observed with the decrease of the instrumental error for the reconstructed 7.458 MeV excitation level in  $^{12}\text{C}$ , which was suggested as the Efimov (Thomas) state.

**Keywords:** heavy ion reactions, Efimov state,  $\alpha$ -particle resonances, relative kinetic energy

**PACS:** 25.70.Pq     **DOI:** 10.1088/1674-1137/43/6/064102

### 1 Introduction

In 1969, Vitaly Efimov, following a work by Thomas (1935) [1], first predicted a puzzling quantum-mechanical effect, when a resonant pairwise interaction gives rise to an infinite number of three-body loosely bound states even though each particle pair is unable to bind [2, 3]. These properties are universal and independent of the details of the short-range interaction when the two-body scattering length ' $a$ ' is much larger than the range of the interaction potential ' $r_0$ '. The existence of resonant two-body forces is the basic condition for the Efimov effect. Although there has been an extensive search in many different physical systems including atoms, molecules and nuclei, experimental confirmation of the existence of Efimov states has proved to be challenging, especially for

nuclei [1-9]. Recently, Tumino et al. reported the discovery of triple-alpha resonances, very close to the Efimov scenario, by studying  $^6\text{Li}+^6\text{Li}\rightarrow 3\alpha$  reactions at low beam energy and using the hyper-spherical formalism. A geometrical interpretation of these mechanisms [10] suggests that the Thomas state corresponds to three equal energies, while a sequential decay mechanism ( $^{12}\text{C}\rightarrow ^8\text{Be}+\alpha\rightarrow 3\alpha$ ) might correspond to Efimov states [2]. This prescription refers mainly to  $^{12}\text{C}$  levels in the vicinity of the breakup threshold of three  $\alpha$ -particles or  $\alpha+^8\text{Be}$ , taking into account the Coulomb force among  $\alpha$ -particles which destroys the  $1/R^2$  ( $R$  is the hyper-radius) scaling at large distances where the Coulomb force is dominant [2]. This is surely relevant for stellar processes, where  $^{12}\text{C}$  nucleus is formed, and it may occur inside a dense star or on its surface, thus in different density and temperature conditions. A way to simulate stellar conditions is to col-

Received 15 January 2019, Published online 8 April 2019

\* Supported by the National Natural Science Foundation of China (11765014, 11605097, 11421505, 11865010), the US Department of Energy (DE-FG02-93ER40773, NNSA DE-NA0003841 (CENTAUR)), and the Robert A. Welch Foundation (A-1266). This work was also supported by the Chinese Academy of Sciences (CAS) President's International Fellowship Initiative (2015VWA070), Strategic Priority Research Program of the Chinese Academy of Sciences (XDB16 and XDPB09), Program for Young Talents of Science and Technology in Universities of Inner Mongolia Autonomous Region (NJYT-18-B21), Doctoral Scientific Research Foundation of Inner Mongolia University for Nationalities (BS365 and BS400), The Fundamental Research Funds for the Central Universities (GK201903022), and Natural Science Foundation of Inner Mongolia (2018MS01009)

1) E-mail: zsytl@imn.edu.cn

©2019 Chinese Physical Society and the Institute of High Energy Physics of the Chinese Academy of Sciences and the Institute of Modern Physics of the Chinese Academy of Sciences and IOP Publishing Ltd

lide two heavy ions with a beam energy near the Fermi energy. In this work, we present the possible signature as the Efimov (Thomas) state of the reconstructed 7.458 MeV excitation level in  $^{12}\text{C}$  from the reactions  $^{70(64)}\text{Zn}(^{64}\text{Ni}) + ^{70(64)}\text{Zn}(^{64}\text{Ni})$  at the beam energy of  $E/A = 35$  MeV/nucleon [11].

## 2 Experiment

The experiment was performed at the Cyclotron Institute, Texas A&M University.  $^{64}\text{Zn}$ ,  $^{70}\text{Zn}$ , and  $^{64}\text{Ni}$  beams at 35 MeV/nucleon from the K-500 superconducting cyclotron were used to respectively irradiate self-supporting  $^{64}\text{Zn}$ ,  $^{70}\text{Zn}$ , and  $^{64}\text{Ni}$  targets. The  $4\pi$  NIMROD-ISiS setup [12, 13] was used to collect charged particles and free neutrons produced in the reactions. A detailed description of the experiment can be found in Refs. [14-16].

When two heavy ions at 35 MeV/nucleon collide, the excitation energy deposited in the system is large enough for the system to be gently compressed in the beginning, after which it expands and enters an instability region, the spinodal region, similar to the liquid-gas (LG) phase transition [17-21]. Fig. 1 shows the time evolution of the average density in the central region  $[-3, 3]^3 \text{fm}^3$  at the incident energy of 35 MeV/nucleon in the collision of  $^{70}\text{Zn} + ^{70}\text{Zn}$  with the Constrained Molecular Dynamics approach (CoMD) [17]. The average density increases in the compression stage and decreases in the expansion stage. The maximum average density reaches around 60 fm/c when the initial distance between projectile and target nuclei is set to 15 fm. In such conditions, fragments of different sizes are formed and can be detected. The NIMROD detector used in this experiment can distinguish charge numbers from 1 to 30 and masses up to 50 [14]. A typical result is plotted in Fig. 2 [14] together with the CoMD results [17], showing a satisfactory agreement with the data. In order to test if some fragments are formed in excited states, an evaporation model, Gemini

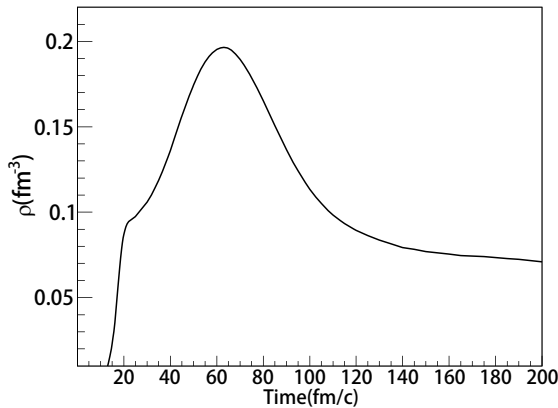


Fig. 1. Time evolution of the average density in the central region in  $^{70}\text{Zn} + ^{70}\text{Zn}$  collision at 35 MeV/nucleon.

[17, 22-25] was applied. The reaction was followed up to a maximum time  $t_{\text{max}}$  in the CoMD model. Within the model, the excitation energy of each fragment formed at  $t_{\text{max}}$  was obtained and fed into the Gemini model, which gives the final de-excited fragments. As can be seen from the figure, the effect of secondary evaporation is negligible after  $t_{\text{max}} > 600$  fm/c. The abundance of  $^{12}\text{C}$  fragments is about two orders of magnitude less than of protons and  $\alpha$ -particles. These ions survive the violence of the collision while other  $^{12}\text{C}$  may be in one of the excited states and decay before reaching the detector, or collide with other fragments and get destroyed. Our technique is tailored to select the  $^{12}\text{C} \rightarrow 3\alpha$  decay channel among all possibilities.

In the experiment, it is straightforward to select all events where one or more  $\alpha$  particles are detected. In Fig. 3, we plot the  $\alpha$ -particle multiplicity distribution for the three colliding systems considered. The total number of events is  $\sim 2.7 \times 10^8$ , and we have observed events where at least 15  $\alpha$ -particles are produced. In Refs. [26-28], an analysis was performed for events shown in Fig. 3 in terms of boson-fermion mixtures, i.e. including all fragments reported in Fig. 2, which can give a signature of the Bose-Einstein Condensation (BEC) [29, 30]. The temperature, density and excitation energy are obtained using different approaches [17], with most of the events in the high excitation energy region up to about 8 MeV/nucleon. We note that most of the novel techniques discussed in this work may be easily generalized to cases where  $\alpha$ -particle multiplicity is larger than 3, which will be the subject of our future paper. A more conventional analysis based on Dalitz plots [31-38] cannot be easily generalized when  $\alpha$ -particle multiplicity is larger than 3.

For the purpose of our work, we further selected all events with only three  $\alpha$ -particles detected. It is important to stress that multiple  $\alpha$ -particles are accepted if they hit different detectors, i.e. all possible double hits in an event are excluded. Furthermore, in the present analysis,

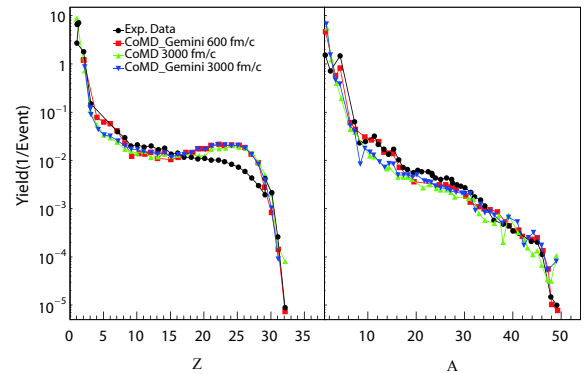


Fig. 2. (color online) Charge ( $Z$ ) and mass ( $A$ ) distributions from the  $^{70}\text{Zn} + ^{70}\text{Zn}$  system are shown for the filtered CoMD simulation and compared to the experimental data. The results are normalized to the total number of events [14].

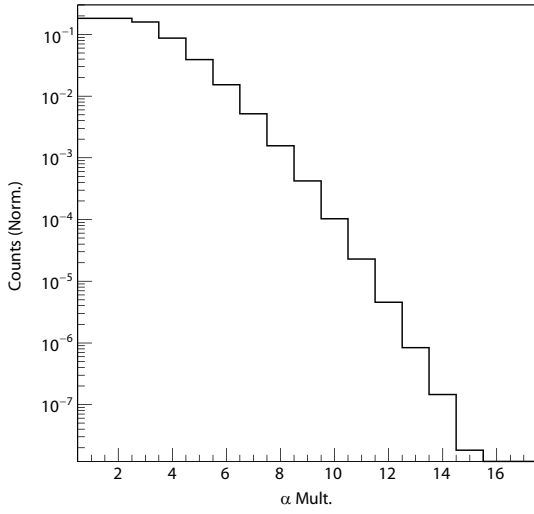


Fig. 3.  $\alpha$ -particle multiplicity distribution from the  $^{70(64)}\text{Zn}(^{64}\text{Ni}) + ^{70}\text{Zn}(^{64}\text{Ni})$  collisions at 35 MeV/nucleon from the NIMROD detector.

a random position on the surface of the detector was assigned to each  $\alpha$ -particle. This limits the precision of  $\alpha$ - $\alpha$  correlations, especially when their relative energies or momenta are very small. A critical comparison of different methods of assigning hit positions in the detector will be discussed in a future work; here, it is sufficient to say that the results discussed are independent of the method used. In our case, the total number of events is reduced to  $\sim 4.5 \times 10^7$ . From the above discussion, it is clear that if only three  $\alpha$ -particles are present in an event, other fragments must be present too and the sum of all fragment masses is 140 (maximum), including the three  $\alpha$ -particles. This is a rich environment in which, depending on their proximity to  $\alpha$ ,  $^8\text{Be}$  or  $^{12}\text{C}$  ions, the properties and shell structure of different fragments may be modified. In particular, short lived states of  $^{12}\text{C}$  or  $^8\text{Be}$  may be modified by the presence of other nearby fragments. On the other hand, long lived states, such as the Hoyle state of  $^{12}\text{C}$ , might not be influenced at all since their lifetime is much longer than the reaction time. Of course, in such a ‘soup’,  $\alpha$ -particles may come from the decay of  $^{12}\text{C}$  or  $^8\text{Be}$ , from different excited fragments, or may be directly produced during the reaction. Thus, it is crucial to implement different methods to distinguish among different decay channels.

In order to distinguish different decay channels, the kinetic energy of  $\alpha$ -particles must be measured with a good precision. The kinetic energy distribution from the NIMROD detector for events with  $\alpha$ -particle multiplicity equal to three is given in Fig. 4. It extends above 100 MeV/nucleon and displays a large yield around 8 MeV/nucleon. Since the kinetic energies are relatively large, the detector is performing at its best, and the error estimate (including the instrumental error, comprising the detector granularity, energy, position, and angle resolu-

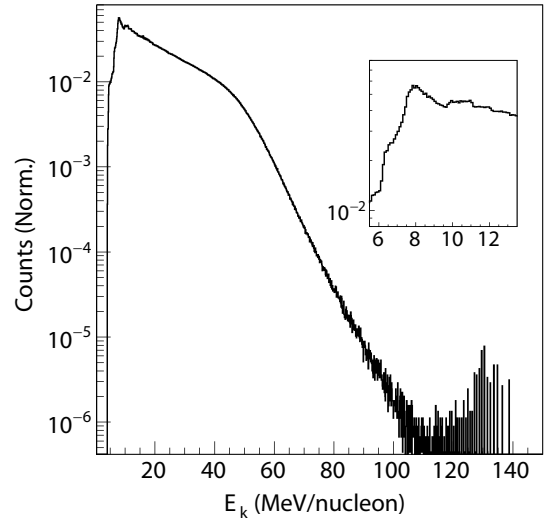


Fig. 4.  $\alpha$ -particle kinetic energy distribution in the laboratory frame from all events with  $\alpha$ -particle multiplicity equal to three. Inset: zoom of the lower energy region.

tion) is less than 1% of the kinetic energy. The error becomes larger for smaller kinetic energies, and particles with kinetic energy below a threshold (about 1 MeV/nucleon) are not detected [14]. Thus, there is a clear advantage to use beams of heavy ions near or above the Fermi energy. The fragments are emitted in the laboratory frame with high kinetic energies (due to the center-of-mass motion) and can be easily detected. When we reconstruct  $^8\text{Be}$  from  $\alpha$ - $\alpha$  correlations, the center-of-mass motion is cancelled out and small relative kinetic energies can be obtained with an estimated error of about 45 keV for the smallest relative kinetic energy. This error is due to the detector granularity as discussed above.

### 3 Method

For a three body system with equal masses, we can define the excitation energy  $E^*$  as:

$$E^* = \frac{2}{3} \sum_{i=1, j>i}^3 E_{ij} - Q \quad (1)$$

where  $E_{ij}$  is the relative kinetic energy of two particles, and  $Q$  is the  $Q$ -value. Note that the important ingredient entering Eq. (1) are the relative kinetic energies; since we have three indistinguishable bosons, we analyze the  $E_{ij}$  distribution by cataloguing for each event the smallest relative kinetic energy,  $E_{ij}^{\text{Min.}}$ , the middle relative kinetic energy,  $E_{ij}^{\text{Mid.}}$ , and the largest relative kinetic energy,  $E_{ij}^{\text{Lar.}}$ .

In this work, we reconstruct the excitation level  $E^* = 7.458$  MeV in  $^{12}\text{C}$  from 3  $\alpha$ -particles when the sum of the three  $E_{ij}$  is 0.276 MeV ( $0.092 \times 3$  MeV, where 0.092 MeV is the relative energy of 2  $\alpha$ -particles corresponding to the ground state decay of  $^8\text{Be}$  [11, 39]) with the  $Q$ -value =

-7.275 MeV. In Fig. 5, the minimum relative kinetic energy distribution is shown. In the top panel, the solid black circles give the distribution obtained from the real events. They show bumps but no real structure. This is due to the fact that in the fragmentation region, some  $\alpha$ -particles may come from the decay of  $^8\text{Be}$  or  $^{12}\text{C}$ , but also from completely non-correlated processes, for example,  $\alpha$ -particle emission from a heavy fragment. To distinguish the correlated from non-correlated events, we randomly choose three different  $\alpha$ -particles from three different events and build the distribution displayed in Fig. 5 (mixing events-red open circles). The total number of real and mixing events is normalized to one. We fit the highest points of Fig. 5 (top) with an exponential function. This allows to derive the instrumental error  $\Delta E = 1/22 \text{ MeV} = 0.045 \text{ MeV}$ . By subtracting the fit function from the real events, we obtain the open squares in Fig. 5 (top), which can be considered as the real events corrected by the detector acceptance. The ratio  $(1+R_3)$  of the real and mixing events is plotted in the bottom of Fig. 5, together with the Breit-Wigner fits. As one can see, the first peak around 0.088 MeV (very close to 0.092 MeV) with a width of 1192 fm/c corresponds to the ground state of  $^8\text{Be}$ , but depends on the detector correction given by the exponential fit. The second peak around 3.05 MeV

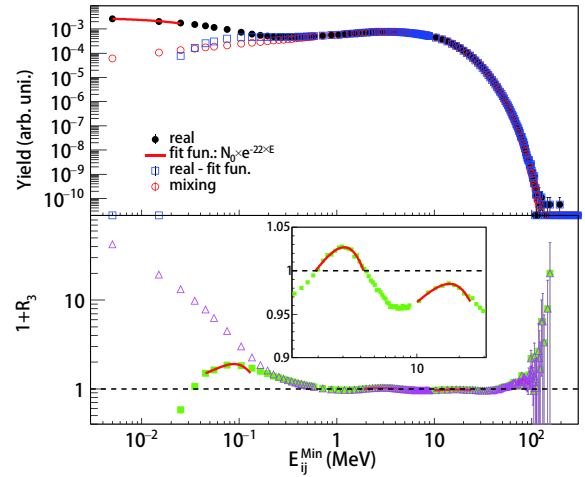


Fig. 5. (color online) (Top) Relative kinetic energy distribution as a function of the minimum relative kinetic energy. The solid black circles represent data from real events, red open circles are from mixing events, and the blue open squares represent the difference between the real events and the exponential fit (solid line), which takes into account the experimental errors. (Bottom) Ratios of the real data (pink open triangles) and the real data minus the fit function (green solid squares) are divided by the mixing events as a function of the minimum relative kinetic energy. Solid lines are the Breit-Wigner fits.

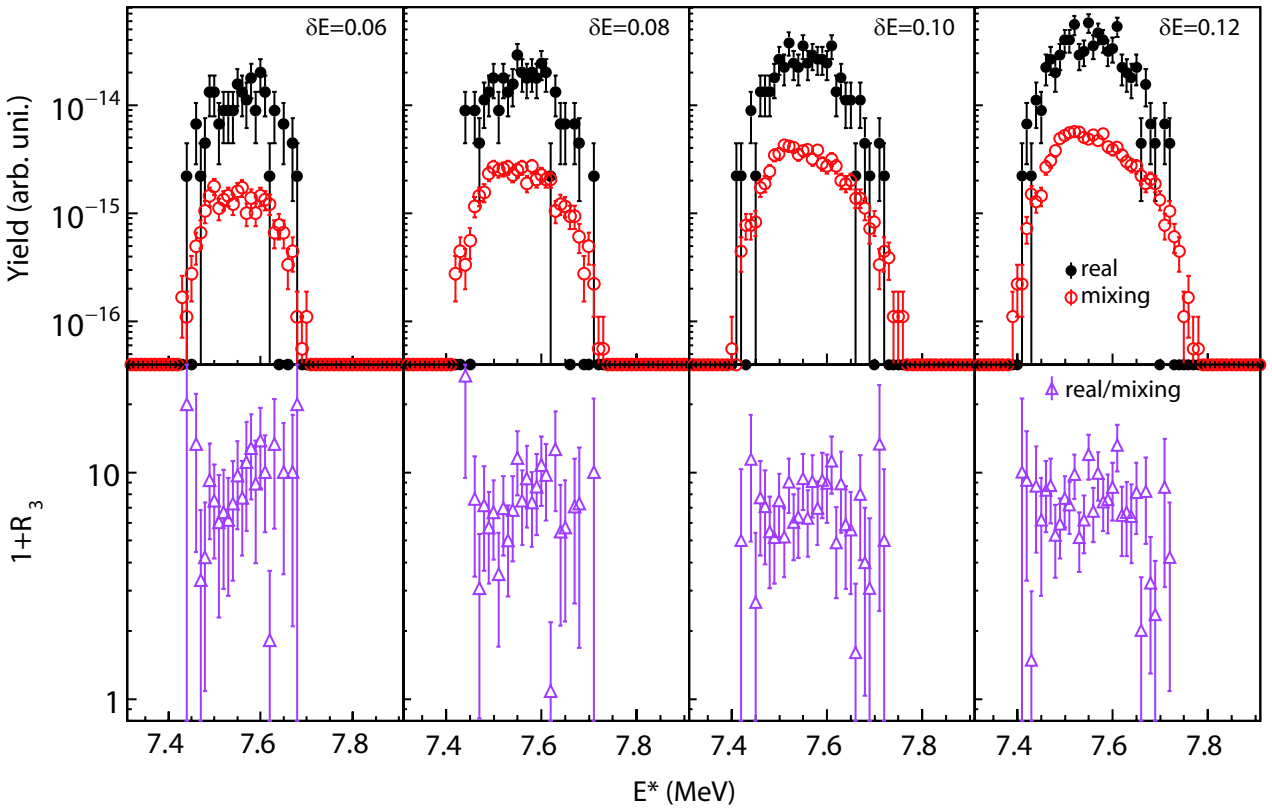


Fig. 6. (color online) Reconstructed excitation energy distributions of  $^{12}\text{C}$  from 3  $\alpha$ -particles with  $E_{ij}^{\text{Min.}} = E_{ij}^{\text{Mid.}} = 0.092 \pm \frac{\delta E}{3} \text{ MeV}$ . The solid black circles are from the real events, red open circles are the mixing events, pink open triangles indicate the ratios of the real events to the mixing events.

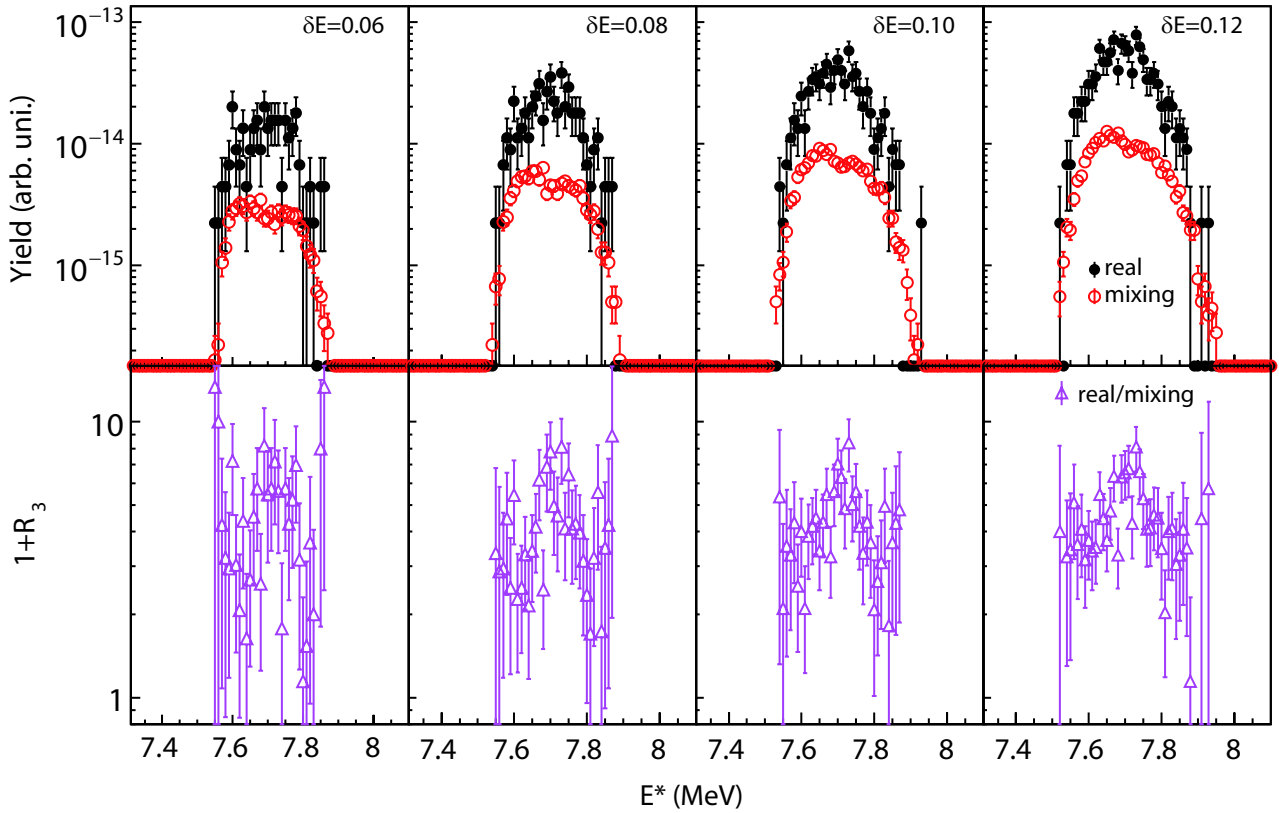


Fig. 7. (color online) Reconstructed excitation energy distributions of  $^{12}\text{C}$  from 3  $\alpha$ -particles with  $E_{ij}^{\text{Min.}} = 0.092 \pm \frac{\delta E}{3}$  MeV,  $E_{ij}^{\text{Mid.}} = 0.092 \times 2 \pm \frac{\delta E}{3}$  MeV. The solid black circles and the red open circles denote respectively the real events and the mixing events, pink open triangles indicate the ratios of the real events to the mixing events.

and a width of 14.2 fm/c (independent of the detector correction) corresponds to the first excited state of  $^8\text{Be}$ . Higher energy peaks above 10 MeV are also visible.

In order to determine if there are events with equal relative kinetic energies, we selected 3  $\alpha$ -particle events with  $E_{ij}^{\text{Min.}} = E_{ij}^{\text{Mid.}} = 0.092 \pm \frac{\delta E}{3}$  MeV and decreased the value of  $\delta E$  to the smallest value allowed by the statistics. In Fig. 6, we plot the results for the real (solid black circles) and the mixing (red open circles) events in the upper panels, and their ratio ( $1+R_3$ ) in the bottom panels. Even though the number of real events decreases to almost 90 when  $\delta E = 0.06$  MeV, we can see a hint of a signal around  $(E_{ij}^{\text{Lar.}} + E_{ij}^{\text{Mid.}} + E_{ij}^{\text{Min.}}) \times \frac{2}{3} - Q \leq 7.47$  MeV, which is consistent with the suggested Efimov (Thomas) state [10, 11, 39] at an excitation energy of about 7.458 MeV in  $^{12}\text{C}$ .

Similar to Fig. 6, we selected 3  $\alpha$ -particle events with  $E_{ij}^{\text{Min.}} = 0.092 \pm \frac{\delta E}{3}$  MeV,  $E_{ij}^{\text{Mid.}} = 0.092 \times 2 \pm \frac{\delta E}{3}$  MeV in Fig. 7. We also observe events where the largest relative energy is three times the minimum one around  $(E_{ij}^{\text{Lar.}} + E_{ij}^{\text{Mid.}} + E_{ij}^{\text{Min.}}) \times \frac{2}{3} - Q = 7.64$  MeV with different  $\delta E$ . These events suggest that there are events where the

3  $\alpha$ -particle relative energies are in the ratio of 1:2:3.

In Figs. 6 and 7, we can see a significant signal around  $E^* = 7.65$  MeV, which is consistent with the famous  $0^+$  Hoyle state of  $^{12}\text{C}$  predicted by Fred Hoyle in 1953 [40].

## 4 Summary

We discussed the Efimov (Thomas) states in excited  $^{12}\text{C}$  nuclei in the reactions  $^{70(64)}\text{Zn}(^{64}\text{Ni}) + ^{70(64)}\text{Zn}(^{64}\text{Ni})$  at the beam energy of  $E/A = 35$  MeV/nucleon. In order to investigate the  $^{12}\text{C}$  states, we analyzed the events with  $\alpha$ -particle multiplicity equal to three. The excitation energies of  $^{12}\text{C}$  were reconstructed by considering the three  $\alpha$ -particle relative kinetic energies. The interaction between any two of the three  $\alpha$ -particles provides events with one, two or three  $^8\text{Be}$  interfering levels. Events with the three relative kinetic energies equal to the ground state energy of  $^8\text{Be}$  are found when decreasing the acceptance width. This may be a signature of the Efimov (Thomas) state in  $^{12}\text{C}$  with the excitation energy of 7.458 MeV. Dedicated experiments with better experimental resolution are suggested in order to exclude any possible experimental effect in the data analysis.



## References

- 1 L. H. Thomas, *Phys. Rev.*, **47**: 903 (1935)
- 2 V. Efimov, *Phys. Lett. B*, **33**: 563 (1970)
- 3 V. Efimov, *Nat. Phys.*, **5**: 533 (2009)
- 4 E. Braaten, H.W. Hammer, *Phys. Rep.*, **428**: 259 (2006)
- 5 A. Tumino, A. Bonasera, G. Giuliani et al, *Phys. Lett. B*, **750**: 59 (2015)
- 6 T. Kraemer, M. Mark, P. Waldburger et al, *Nature*, **440**: 315 (2006)
- 7 M. Zaccanti, B. Deissler, C. D'Errico et al, *Nat. Phys.*, **5**: 586 (2009)
- 8 Bo Huang et al, *Phys. Rev. Lett.*, **112**: 190401 (2014)
- 9 M. Gattobigio and A. Kiewsky, *Phys. Rev. A*, **90**: 012502 (2014)
- 10 H. Zheng and A. Bonasera, arXiv: 1811.10412
- 11 S. Zhang et al., arXiv: 1810.01713
- 12 S. Wuenschel et al, *Nucl. Instrum. Methods A*, **604**: 578 (2009)
- 13 R. Schmitt et al, *Nucl. Instrum. Methods A*, **354**: 487 (1995)
- 14 Z. Kholey, 2010 PhD Thesis Texas A&M University
- 15 Z. Kohley et al, *Phys. Rev. C*, **83**: 044601 (2011)
- 16 Z. Kohley et al, *Phys. Rev. C*, **86**: 044605 (2012)
- 17 G. Giuliani et al, *Prog. Part. Nucl. Phys.*, **76**: 116 (2014)
- 18 A. Bonasera, F. Gulminelli and J. Molitoris, *Phys. Rep.*, **243**: 1 (1994)
- 19 Y.G. Ma, *Phys. Rev. Lett.*, **83**: 3617 (1999)
- 20 Y.G. Ma, J. B. Natowitz, R. Wada et al, *Phys. Rev. C*, **71**: 054606 (2005)
- 21 C. W. Ma and Y. G. Ma, *Prog. Part. Nucl. Phys.*, **99**: 120 (2018)
- 22 Y.G. Ma, R. Wada, K. Hagel et al, *Phys. Rev. C*, **65**: 051602(R) (2002)
- 23 Z. F. Zhang, D. Q. Fang, and Y. G. Ma, *Nucl. Sci. Tech.*, **29**: 78 (2018)
- 24 W. D. Tian, Y. G. Ma, Z. X. Cai et al, *Chinese Phys. C*, **30**(S2): 280 (2006)
- 25 X. Jiang and N. Wang, *Chinese Phys. C*, **42**(10): 104105 (2018)
- 26 P. Marini et al. [INDRA Collaboration], *Phys. Lett. B*, **756**: 194 (2016)
- 27 K. Schmidt et al, *Phys. Rev. C*, **95**: 054618 (2017)
- 28 J. Mabiola, H. Zheng, A. Bonasera et al, *Phys. Rev. C*, **94**: 064617 (2016)
- 29 A. Tohsaki, H. Horiuchi, P. Schuck et al, *Phys. Rev. Lett.*, **87**: 192501 (2001)
- 30 Y. Funaki, T. Yamada, H. Horiuchi et al, *Phys. Rev. Lett.*, **101**: 082502 (2008)
- 31 M. Freer et al, *Phys. Rev. C*, **49**: R1751 (1994)
- 32 Ad. R. Raduta et al, *Phys. Lett. B*, **705**: 65 (2011)
- 33 J. Manfredi et al, *Phys. Rev. C*, **85**: 037603 (2012)
- 34 O. S. Kirsebom et al, *Phys. Rev. Lett.*, **108**: 202501 (2012)
- 35 T. K. Rana et al, *Phys. Rev. C*, **88**: 021601 (2013)
- 36 M. Itoh et al, *Phys. Rev. Lett.*, **113**: 102501 (2014)
- 37 R. Smith et al, *Phys. Rev. Lett.*, **119**: 132502 (2017)
- 38 D. Dell'Aquila et al, *Phys. Rev. Lett.*, **119**: 132501 (2017)
- 39 H. Zheng, A. Bonasera, M. Huang et al, *Phys. Lett. B*, **779**: 460 (2018)
- 40 F. Hoyle, *Astrophys. J. Suppl. Ser.*, **1**: 121 (1954)